SHOCK, Vol. 57, No. 3, pp. 344–350, 2022

OPEN

UAMC-3203 OR/AND DEFEROXAMINE IMPROVE POST-RESUSCITATION MYOCARDIAL DYSFUNCTION THROUGH SUPPRESSING FERROPTOSIS IN A RAT MODEL OF CARDIAC ARREST

Tao Jin,[*†‡] Qing He,[*§] Cheng Cheng,[‡] Hui Li,[‡] Lian Liang,[‡] Guozhen Zhang,[‡] Chenglei Su,[‡] Yan Xiao,[‡] Jennifer Bradley,[‡] Mary Ann Peberdy,[‡‖] Joseph P. Ornato,[‡¶] and Wanchun Tang[‡¶]

[*]School of Materials Science and Engineering, Southwest Jiaotong University, Chengdu, Sichuan Province, China; [†]School of Medicine, Anhui University of Science & Technology, Huainan, Anhui Province, China; [‡]Weil Institute of Emergency and Critical Care Research, Virginia Commonwealth University, Richmond, Virginia; [§]Third People's Hospital of Chengdu Affiliated to Southwest Jiaotong University, Chengdu, Sichuan Province, China; [‖]Departments of Internal Medicine and Emergency Medicine, Virginia Commonwealth University Health System, Richmond, Virginia; and [¶]Department of Emergency Medicine, Virginia Commonwealth University Health System, Richmond, Virginia

Received 9 Jun 2021; first review completed 28 Jun 2021; accepted in final form 22 Sep 2021

ABSTRACT—Blocking ferroptosis reduces ischemia-reperfusion injury in some pathological contexts. However, there is no evidence that ferroptosis contributes to post-resuscitation myocardial dysfunction (PRMD). Here, we evaluated the therapeutic performance of ferroptosis inhibitors (UAMC-3203 or/and Deferoxamine) on the PRMD in a rat model of cardiac arrest and surveyed the changes of essential ferroptosis markers in the myocardium. Remarkably, all treatments reduce the severity of cardiac dysfunction and microcirculation hypoperfusion after resuscitation compared with control. Consistently, we observe that the ferroptosis marker Glutathione peroxidase 4, 4-hydroxynonenal and non-heme iron altered (1 ± 0.060 vs. 0.021 ± 0.016, 1 ± 0.145 vs. 3.338 ± 0.221, 52.010 ± 3.587 ug/g vs. 70.500 ± 3.158 ug/g, all $P < 0.05$) in the myocardium after resuscitation. These changes were significantly suppressed by UAMC-3203 [(0.187 ± 0.043, 2.848 ± 0.169, all $P < 0.05$), (72.43 ± 4.920 ug/g, $P > 0.05$)], or Deferoxamine (0.203 ± 0.025, 2.683 ± 0.273, 55.95 ± 2.497 ug/g, all $P < 0.05$). Briefly, UAMC-3203 or/and Deferoxamine improve post-resuscitation myocardial dysfunction and provide evidence of ferroptosis involvement, suggesting that ferroptosis inhibitors could potentially provide an innovative therapeutic approach for mitigating the myocardial damage caused by cardiopulmonary resuscitation.

KEYWORDS—Deferoxamine, ferroptosis, myocardial dysfunction, post-resuscitation, treatment, UAMC-3203

INTRODUCTION

In the United States, there are about 360,000 out-of-hospital cardiac arrest (CA) cases that occur annually (1). Mortality after performing cardiopulmonary resuscitation (CPR) in out-of-hospital CA remains high, and post-resuscitation myocardial dysfunction (PRMD) is considered as one of the main causes of early death (2). Nevertheless, the mechanisms responsible for PRMD are still not well understood.

Critical pathogenesis in the development of fatal cardiac injury is the demise of terminally differentiated cardiomyocytes. Ferroptosis is a newly identified type of regulated cell death marked by the lethal increase of iron-dependent lipid peroxides (3, 4). The amount of redox-active iron, the oxidation level of polyunsaturated fatty acids, and the depletion of repair capability for lipid peroxidation (LPO) by glutathione peroxidase 4 (GPX4) are the three most principal ferroptotic markers and are necessary for the occurrence of ferroptosis (5). To date, ferroptosis has been shown to be involved in the pathological processes associated with carcinogenesis, stroke, and degenerative diseases (4). Recent literature suggests that ferroptosis is also responsible for ischemia/reperfusion injury (IRI) in the liver or kidney (6–8). Besides, it has been reported that ferroptosis might be a mechanism of ischemia/reperfusion (I/R)-induced cardiomyopathy in various models (9, 10). IRI is a significant contributor to the pathology of PRMD. However, definitive evidence linking the mechanism of PRMD to ferroptosis is currently lacking.

UAMC-3203 is a novel drug-like ferroptosis inhibitor improved from analogs of ferrostatin-1. It shows more potent protection against *in vivo* multi-organ injury by its radical trapping properties (11). Deferoxamine (DFO) is an iron chelator used to treat diseases with iron overload in the past. It has been reported that DFO has a neuroprotective and cardioprotective effect, but its underlying mechanism remains unclear (12). Recently, DFO was identified as a ferroptosis inhibitor for the study of cell death (3). In the present study, we hypothesize that ferroptosis plays a critical role in PRMD. The ferroptosis-specific inhibitor may promote protection and repair on myocardial function following CPR.

Address reprint requests to Qing He, MD, PhD, Department of Emergency, Third People's Hospital of Chengdu Affiliated to Southwest Jiaotong University, Chengdu, Sichuan Province 610031, China. E-mail: 123hq@163.com; Co-correspondence: Wanchun Tang, MD, MCCM, FAHA, FNAI, Weil Institute of Emergency and Critical Care Research at VCU, Box 980266, Sanger Hall, 1101 E Marshall St, Richmond, VA 23298-0279. E-mail: wanchun.tang@vcuhealth.org

TJ and QH contributed equally to this work.

This study was supported, in part, by the Weil family foundation, CA.

The authors report no conflicts of interest.

DOI: 10.1097/SHK.0000000000001869

MATERIALS AND METHODS

This study was conducted according to a protocol (AD10001396-22) approved by the Institutional Animal Care and Use Committee (IACUC) of Virginia Commonwealth University. All animals received humane care in full compliance with the Guide for the Care and Use of Laboratory Animals published by the National Institutes of Health. Data and other materials supporting this study are available from the corresponding author on reasonable request.

Animal preparation

Male Sprague-Dawley rats (450 g–550 g) were purchased from Envigo (Frederick, Md). Animals were kept under standard conditions with a 12/12-h day/night cycle and received food and water *ad libitum*. Following induction with inhaling low flow CO_2 for 30 s, animals were anesthetized by intraperitoneal injection of pentobarbital (45 mg/kg). Additional doses (10 mg/kg) were administered as needed based on tail pinch/withdrawal reflex to maintain anesthesia. This study was approved to be conducted without analgesia by the IACUC. Tracheal intubation was performed orally and connected to a side-stream infrared CO_2 analyzer (Capstar-100 Carbon Dioxide Analyzer; CWE, Ardmore, Pa) to monitor End-tidal CO_2 ($ETCO_2$).

A conventional lead II electrocardiogram (ECG) was gauged continuously. For the measurement of the blood temperature, a thermocouple microprobe (IT-18; Physitemp Instruments, Clifton, NJ) was advanced into the left femoral vein. The blood temperature was maintained at 37°C ± 0.5°C by a heated surgical board. A polyethylene catheter (PE-50; Becton Dickinson, Sparks, Md) was inserted from the left femoral artery into the descending aorta to monitor arterial pressure and withdraw blood. Another PE-50 catheter was advanced through the left external jugular vein into the right atrium to measure the right atrial pressure (RAP). Through the right external jugular vein, a 3F catheter (Model C-PMS-301J; Cook Critical Care, Bloomington, Ind) was inserted into the right atrium. A precurved guidewire was advanced through this catheter into the right ventricle to induce ventricular fibrillation (VF). The endocardial electrocardiograph was used to confirm placement of the guidewire. All catheters were flushed intermittently with a saline solution containing 2.5 IU/mL crystalline bovine heparin.

CA model

Experiments were performed from a previously described rat model of cardiac arrest and cardiopulmonary resuscitation (13, 14). Fifteen minutes before inducing VF, baseline measurements including hemodynamic parameters, sublingual microcirculation, and echocardiography were obtained. Mechanical ventilation was performed at a frequency of 100 breaths/min, an inspired O_2 fraction (FiO_2) of 21% and a tidal volume of 0.60 mL/100 g body weight. After 10 min, mechanical ventilation was off-line, and VF was induced through the guidewire, by which a current with a frequency of 60 Hz and gradually increasing intensity with a maximum of 3.5 mA was delivered to the right ventricular endocardium. The electric current lasted for 3 min to avoid spontaneous defibrillation. After 6 min of untreated VF, precordial compression (PC) was begun at a rate of 200/min by a pneumatically powered mechanical chest compressor, to run concurrently with mechanical ventilation (frequency 100 breaths/min, FiO_2 100%, tidal volume 0.60 mL/100 g body weight), by an equal compression/relaxation ratio of 1:1 and a compression/ventilation ratio of 2:1 for 8 min. The depth of compression was adjusted in time for keeping coronary perfusion pressure (CPP) at 22 ± 2 mm Hg. Following CPR, defibrillation was initiated with up to 4-J counter shocks. The criteria used for assessing return of spontaneous circulation (ROSC) were recovery of supraventricular rhythm and a mean aortic pressure higher than 50 mm Hg for 5 min. In case ROSC was not acquired, another PC was resumed for 30 s, followed by the next defibrillation attempt (up to three cycles). After successful resuscitation, animals were closely monitored for 6 h, during which FiO_2 was gradually adjusted from 100% of the first hour to 50% of the second hour and 21% thereafter.

Experimental protocol

Animals were randomized into five groups (n = 6 per group): Sham, Control, UAMC-3203, DFO, UAMC-3203 + DFO. Sham underwent exactly the same surgical procedures as the other groups except without VF and CPR. Five groups were administered with UAMC-3203 (Selleckchem, S8792, 5 mg/kg, 1 mg/mL), DFO (Cayman, 14595, 100 mg/kg, 100 mg/mL) or/and corresponding placebo (2%DMSO, saline) by intraperitoneal injection at the start of PC. Investigators involved in CPR were blinded to the group assignments.

At 6 h after ROSC, the rats were euthanized by an intravenous injection of Euthasol (A commercial euthanasia solution containing pentobarbital sodium and phenytoin sodium, 150 mg/kg). The heart was rapidly harvested and frozen in liquid nitrogen for further assay. A routine necropsy was performed to determine whether there were gross abnormalities, including traumatic injuries caused by cannulation, airway management, surgical operation, or precordial compression.

Hemodynamics measurements

Heart rate, ECG, mean aortic pressure, RAP, blood temperature, and $ETCO_2$ were continuously recorded by a WINDAQ data-acquisition system (DATAQ, Akron, Ohio). CPP was calculated via diastolic aortic pressure minus right atrial pressure displayed on the screen in real time.

Echocardiography

To estimate myocardial function, ejection fraction (EF), cardiac output (CO), and myocardial performance index (MPI) were examined by echocardiography (HD11XE; Philips Medical Systems, Eindhoven, The Netherlands) at baseline, 15 min, 1, 3, and 6 h post-ROSC. All data were collected and reviewed separately by observers blinded to the groups.

Sublingual microcirculation

Sublingual microcirculation was visualized on a side-stream dark-field imaging device (MicroScan; MicroVision Medical, Amsterdam, The Netherlands) with an on-screen magnification of 276 × at baseline, 15 min, 1, 3, and 6 h after ROSC. Microcirculatory flow index (MFI) and perfused vessel density (PVD) were calculated as previously published (15, 16). After the image was divided into four quadrants, observers blinded to the groups independently graded each quadrant from 0 to 3 by a semiquantitative flow score according to the predominant type of flow (0 = no flow, 1 = intermittent, 2 = sluggish, 3 = normal). MFI = the average values of four quadrants. Then we partitioned the image with three calibrated grids of vertical and horizontal lines and calculated the capillary density as the total number of small (<20 um) vessels crossing the lines of the grid divided by the total length of the lines. PVD = the number of perfused vessel/the total length of the lines (1/mm). We averaged discrete scores from each of the three video segments to give a value of flow state for each time point.

Western blot

Heart tissues were collected at 6 h post-ROSC and lysed by homogenization in radio immunoprecipitation assay buffer containing protease inhibitor cocktail (Roche). Homogenates were centrifuged at 12,000 rpm at 4°C for 15 min, and supernatants were extracted for later use. 30 ug of protein for each sample was loaded on a 4% to 20% sodium dodecyl sulfate/polyacrylamide gel eletrophoresis (SDS/PAGE) gel for electrophoresis and transferred to a polyvinylidene difluoride membrane. The membranes were blocked in 1 × Tris Buffer Saline with 1% Casein at room temperature on a shaker for 1 h. Subsequently, the membranes were incubated with primary antibodies against GPX4 (Ab#125066, Abcam, Cambridge, MA, USA), 4-HNE (Ab#46545, Abcam, Cambridge, MA, USA) and glyceraldehyde-3-phosphate dehydrogenase (GAPDH) (Ab#8245, Abcam, Cambridge, MA, USA) at 4°C overnight. Following washing with 1 × TBS with Tween, the membranes were incubated with secondary anti-rabbit/mouse IgG at room temperature for 1 h. Quantitation of the target proteins was analyzed using ImageJ software. Before statistical evaluation, all grayscale values were normalized by GAPDH.

Iron content

Heart tissue collected at 6 h after ROSC was homogenized sitting on ice. Iron levels were measured using an iron assay kit (Ab#83366, Abcam, USA). Outputs were read at optical density (OD) 593 nm on iMark Microplate Reader (BIO-RAD) and the iron content in samples was then determined by comparing the OD of the samples to the standard curve. Results were presented as micrograms of iron per gram of wet tissue weight.

Statistical analysis

Statistical analysis was performed with SPSS 22.0 for windows (SPSS Inc, Chicago, Ill). All data were presented as mean ± SD after testing of normality of distribution by Kolmogorov–Smirnov. ANOVA with Tukey *post hoc* test was employed for measurements among groups. Comparisons between each group including measurements at different time points were analyzed with repeated-measurement ANOVA. Non-normal data were analyzed by the Kruskal–Wallis. A value of P less than 0.05 was regarded as statistically significant.

RESULTS

Baseline parameters and CPR characteristics

A total of 36 rats were used in this study, six rats were excluded from the experiment due to malfunction of

instrumentation during preparation (2/6) or failure during CPR (4/6). Finally, the remaining 30 rats were successfully resuscitated and included in analysis. There were no significant differences in hemodynamic and physiological parameters at baseline among five groups (Table 1). No apparent differences were observed in some characteristics during CPR between control and several treatment groups (Table 1).

UAMC-3203 or/and DFO improved post-resuscitation myocardial dysfunction

To address whether treatment with ferroptosis inhibitors ameliorates myocardial dysfunction after resuscitation, we conducted ultrasound measurements at baseline, 15 min, 1, 3, and 6 h after ROSC. As shown in (Fig. 1 A–C), myocardial function was significantly impaired after resuscitation. In contrast to the control group, UAMC-3203 or/and DFO remarkably improved EF, CO, and MPI at 1, 3, and 6 h after ROSC, except that CO was increased 2 h later in the DFO group. The combined treatment was only more effective than DFO at certain time points, and there was no difference between combination and UAMC-3203. Additionally, the UAMC-3203 group was significantly superior to the DFO group for CO.

UAMC-3203 or/and DFO ameliorated post-resuscitation sublingual microcirculation

To further evaluate cardiac function from the peripheral blood supply, we used MicroScan to examine the sublingual microcirculation at baseline, 15 min, 1, 3, and 6 h after ROSC. After successful resuscitation, the perfusion of sublingual microcirculation showed apparent deficiency at all time points (Fig. 2 A–C). Treatment with UAMC-3203 or/and DFO significantly attenuated microcirculation impairment when compared with the control group. Furthermore, the UAMC-3203 + DFO took effect earlier than the UAMC-3203 or DFO group, and the combination showed better therapy from 3 to 6 h post-ROSC. Like echocardiography, there was a dramatic difference in the therapeutic effect on sublingual microcirculation between the UAMC-3203 and DFO, but on the contrary, DFO improved microcirculation more obviously than UAMC-3203.

UAMC-3203 or/and DFO alleviated the changes of critical molecules in the ferroptosis pathway induced by CPR

To validate whether ferroptosis is involved, we detected the GPX4 and 4-HNE modified proteins at 6 h after ROSC by western blot (Fig. 3A). As expected, GPX4 showed a noticeable decrease after resuscitation (Fig. 3B). After treatment with UAMC-3203 or/and DFO, the expression of GPX4 was upregulated and increased even further in the combination group. On the contrary, 4-HNE modified proteins were increased after resuscitation and were markedly decreased in all treatment groups (Fig. 3C). Compared with the UAMC-3203 or DFO alone, the combined group significantly reduced the 4-HNE modified proteins' level.

DFO mitigated the cardiac non-heme iron overload induced by CPR

Furthermore, to assess post-resuscitation iron overload, the total non-heme iron level of cardiac tissue at 6 h after ROSC was detected by the assay kit (Fig. 4). Similar to LPO, non-heme iron accumulated significantly in the myocardium after resuscitation. DFO or UAMC-3203 + DFO treatment remarkably lowered cardiac non-heme iron content, whereas UAMC-3203 did not work.

DISCUSSION

The present study demonstrated that treatment with ferroptosis inhibitor, UAMC-3203 or/and DFO, reduced severity of myocardial dysfunction, and we further found that GPX4 and 4-HNE were significantly changed after CPR. Notably, inhibiting ferroptosis with UAMC-3203 remarkably reduced these trends, similar to the protective effects of iron chelation by DFO,

Table 1. **Baseline parameters and CPR characteristics of all rats**

Variables	Sham (n = 6)	Control (n = 6)	UAMC-3203 (n = 6)	DFO (n = 6)	UAMC-3203 + DFO (n = 6)	*P*
Body weights (g)	474 ± 25	478 ± 16	491 ± 30	496 ± 19	491 ± 21	0.402
Blood temperature (°C)	36.9 ± 0.3	36.8 ± 0.3	36.7 ± 0.3	36.8 ± 0.3	36.7 ± 0.2	0.742
Heart rate (bpm)	394 ± 27	400 ± 23	393 ± 17	381 ± 16	398 ± 27	0.647
MAP (mm Hg)	123 ± 10	132 ± 9	131 ± 11	129 ± 7	132 ± 8	0.382
PC depth (mm)	N/A	13 ± 1	12 ± 2	13 ± 1	12 ± 1	0.278
No. of shocks	N/A	1.8 ± 0.8	1.5 ± 0.8	2.2 ± 1.2	2.5 ± 1.0	0.339
CPP (mm Hg)						
PC2	N/A	26.9 ± 2.1	26.3 ± 2.2	27.3 ± 1.5	27.0 ± 2.3	0.859
PC4	N/A	26.5 ± 1.1	25.7 ± 0.9	26.7 ± 2.0	27.2 ± 1.6	0.376
PC6	N/A	27.6 ± 2.4	27.4 ± 1.8	27.8 ± 1.7	26.4 ± 1.9	0.623
$ETCO_2$ (mm Hg)						
BL	39.1 ± 2.8	37.8 ± 2.5	40.1 ± 2.8	39.1 ± 3.1	39.7 ± 3.1	0.696
PC2	N/A	17.1 ± 2.0	18.0 ± 2.5	16.5 ± 1.7	17.5 ± 1.5	0.606
PC4	N/A	17.6 ± 1.4	18.7 ± 1.8	17.8 ± 1.9	17.2 ± 2.0	0.533
PC6	N/A	17.9 ± 2.3	18.3 ± 2.6	17.0 ± 2.1	17.8 ± 2.2	0.800

Data were presented as means ± SD.
CPP indicates coronary perfusion pressure; CPR, cardiopulmonary resuscitation; DFO, deferoxamine; $ETCO_2$, end-tidal CO_2; MAP, mean artery pressure; PC, precordial compression; PCn, n minute after PC.
All variables were compared with one-way ANOVA, $P > 0.05$. The CPR values in the sham group were expressed as N/A due to no CA.

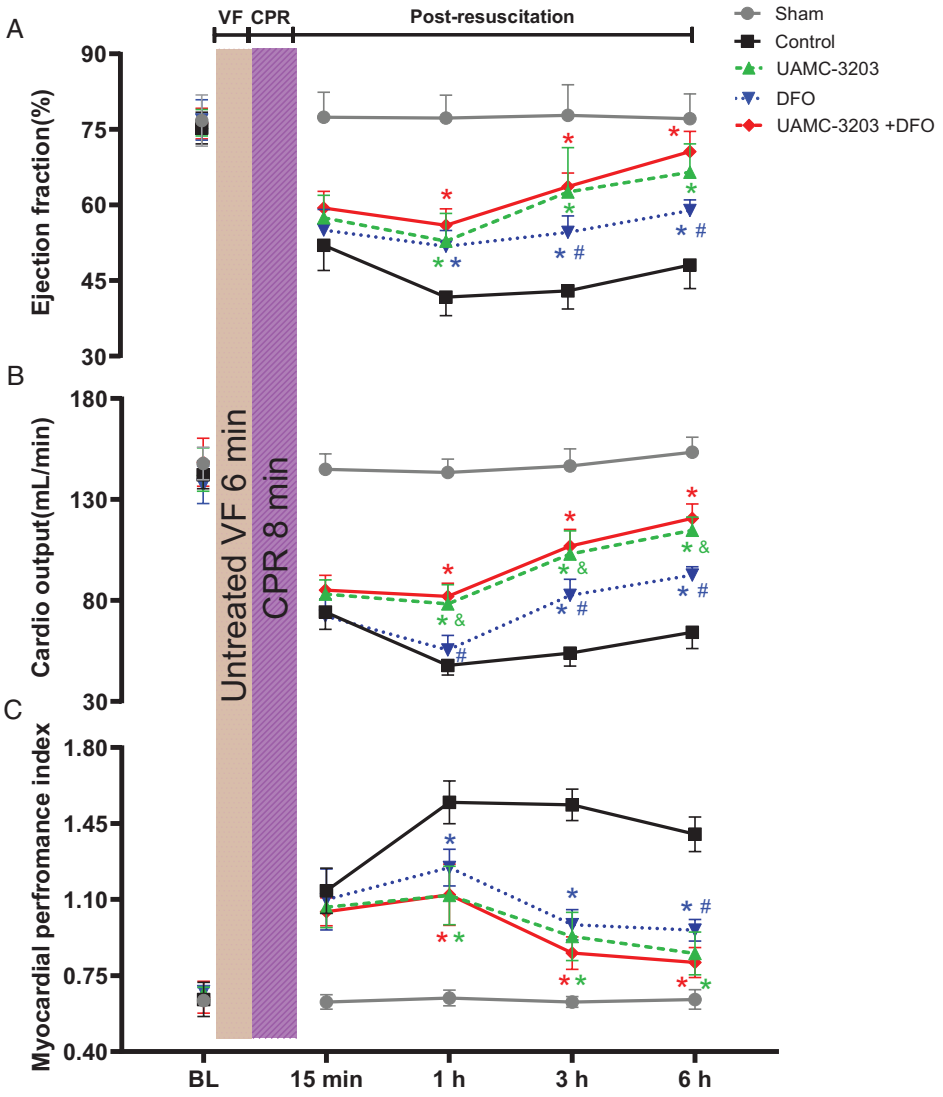

Fig. 1. **Effects of UAMC-3203, DFO, and UAMC-3203 combined with DFO on post-resuscitation myocardial dysfunction.** (A) Ejection fraction, (B) cardiac output, (C) myocardial performance index. Data are measured by echocardiography, and results are presented as the mean ± SD (n = 6 per group). Comparisons between multiple groups were made using repeated-measurement analysis of variance. * with different colors represent the group with the corresponding color versus control group ($P < 0.05$). # with different colors represent the group with the corresponding color versus UAMC-3203 combined with DFO group ($P < 0.05$). & represent UAMC-3203 versus the DFO group ($P < 0.05$). BL indicates baseline; CPR, cardiopulmonary resuscitation; DFO, deferoxamine; VF, ventricular fibrillation.

suggesting ferroptosis might be involved in PRMD. Moreover, DFO decreased post-resuscitation iron overload observed in heart tissue. Therefore, we inferred that UAMC-3203 and DFO alleviated myocardial dysfunction via inhibiting ferroptosis, which could be a novel possible target for PRMD treatment.

This is the first attempt to use ferroptosis inhibitors in the treatment of PRMD, and we found that UAMC-3203 or/and DFO improved cardiac function after ROSC. Although these two drugs block ferroptosis by distinct mechanisms, the combination had no synergy effects. Furthermore, the efficacy of UAMC-3203 was better than that of DFO only in CO. Both CO and EF are used to estimate myocardial contractility, while MPI is affected by myocardial systolic and diastolic function. Their inconsistency on echocardiography may have caused this distinction.

The sublingual microcirculation state is also an important parameter reflecting severity of PRMD (17). We observed that both UAMC-3203 and DFO could recover sublingual microcirculation perfusion, consistent with cardiac function. Paradoxically, the effect of DFO was significantly better than that of UAMC-3203 in both microcirculation indexes. Except for cardiac output, many other factors affecting microcirculation, such as microvascular diameter, endothelial function, local vasoactive substances, and blood state, might be responsible for the inconsistency. Hemodynamics did not show that two ferroptosis inhibitors had significant direct vasoactive effects in this experiment. Besides, the no-reflow phenomenon also hinders microcirculatory reperfusion after CA or shock, and LPO during I/R is supposed to be associated with such parafunction. DFO has been reported to significantly increase early cerebral perfusion after resuscitation in rats by inhibiting LPO activation (18). We think this is the possible reason DFO presented a better performance on ameliorating microcirculation. On the other hand, a recent study (19) suggested that DFO increased the rAQP4 level in the brain by reducing Fe^{2+}

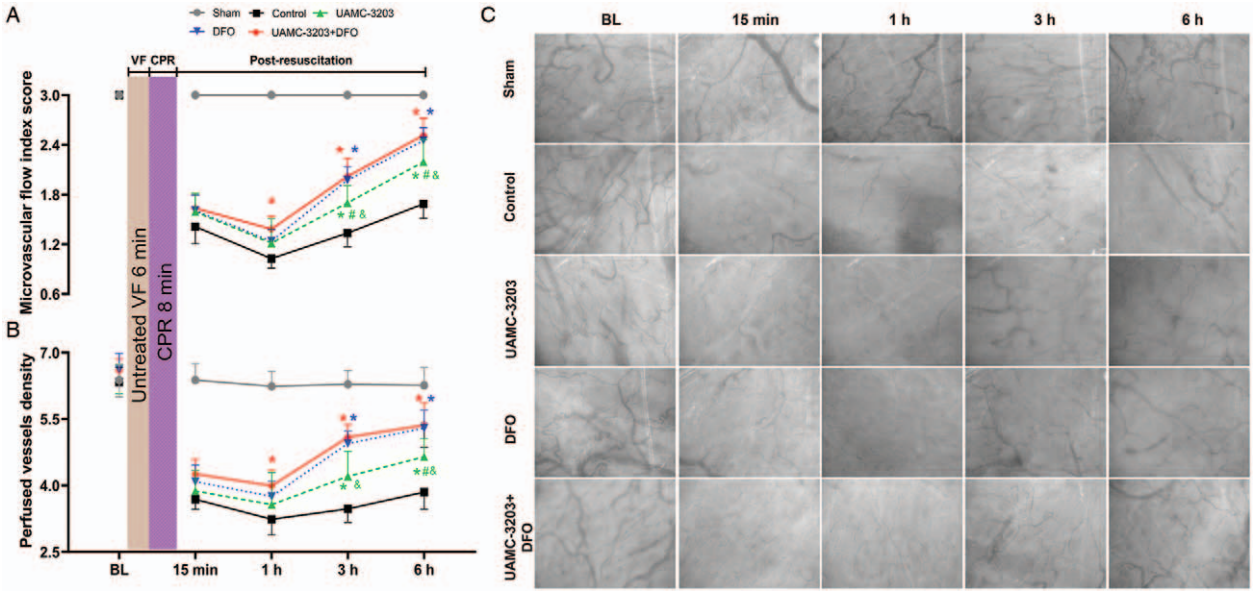

Fig. 2. **Effects of UAMC-3203, DFO, and UAMC-3203 combined with DFO on post-resuscitation sublingual microcirculation.** (A) Microvascular flow index score, (B) perfused vessel density, (C) representative digital photomicrographs of sublingual microcirculation. Data are measured by the Microscan imaging device (n = 6 per group). Results are shown as the mean ± SD. Comparisons between multiple groups were made using repeated-measurement analysis of variance. * with different colors represent the group with the corresponding color versus control group ($P < 0.05$). # with different colors represent the group with the corresponding color versus UAMC-3203 combined with DFO group ($P < 0.05$). & represent UAMC-3203 versus DFO group ($P < 0.05$). BL indicates baseline; CPR, cardiopulmonary resuscitation; DFO, deferoxamine; VF, ventricular fibrillation.

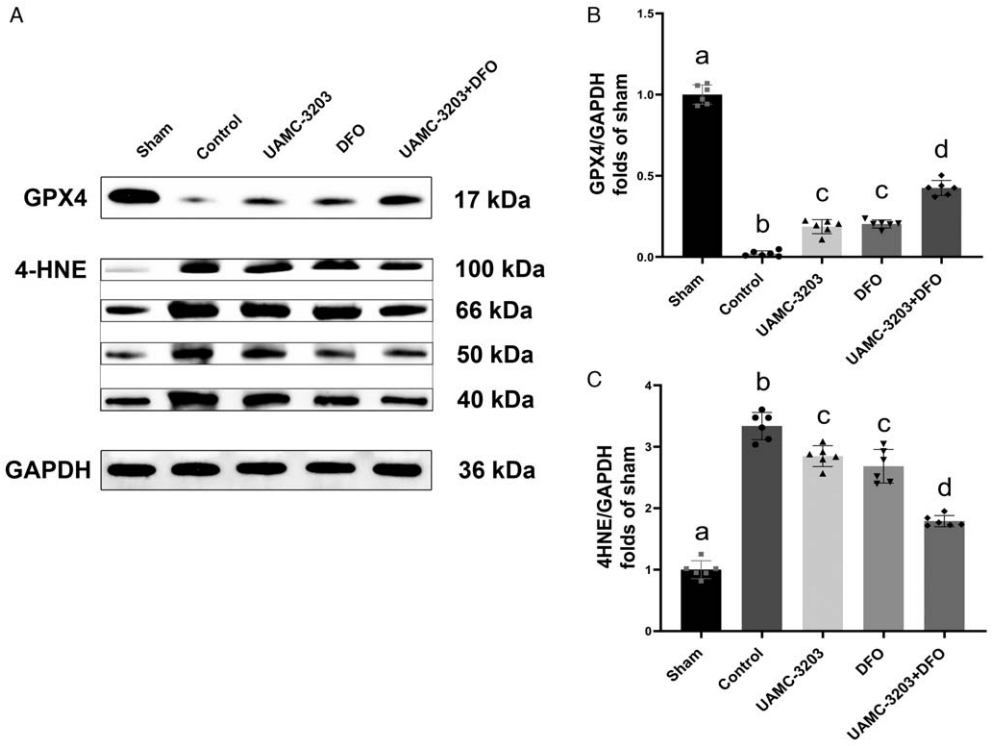

Fig. 3. **Characterization of ferroptosis pathway following CPR.** A, Expressions of GPX4 and 4-HNE modified proteins in the heart were evaluated by western blotting at 6 h post-ROSC (n = 6 per group). B and C, Quantification of GPX4 and 4-HNE modified proteins expressions. Band intensities were analyzed by using ImageJ software and normalized to GAPDH. Data are shown as mean ± SD. Comparisons between multiple groups were made by one-way ANOVA with Tukey *post hoc* test. Groups labeled with unlike letters were significantly different ($P < 0.05$). 4-HNE indicates 4-hydroxynonenal; DFO, deferoxamine; GAPDH, glyceraldehyde-3-phosphate dehydrogenase; GPX4, glutathione peroxidase 4.

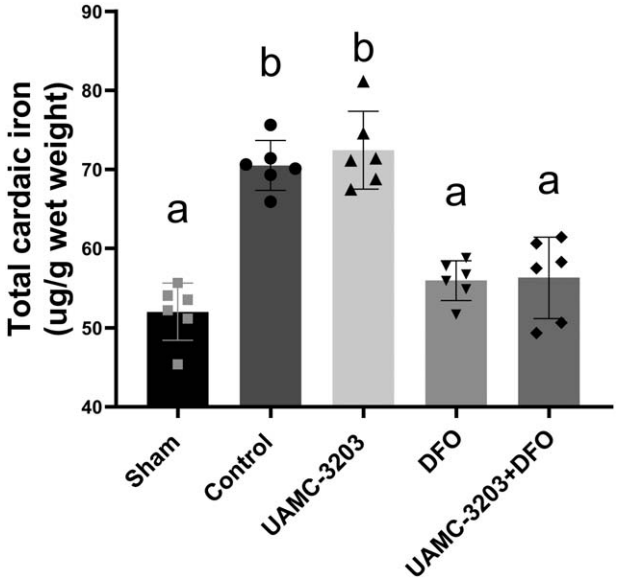

Fig. 4. **Effects of UAMC-3203, DFO, and UAMC-3203 combined with DFO on cardiac iron content post-resuscitation.** Iron levels in the heart were detected by the iron assay kit at 6 h post-ROSC (n = 6 per group). Data are shown as mean ± SD. Comparisons between multiple groups were made using one-way ANOVA with Tukey *post hoc* test. Groups labeled with unlike letters were significantly different ($P < 0.05$). DFO indicates deferoxamine.

content, which raised another possibility that DFO could change local microcirculation by the osmotic load.

GPX4 is an essential negative regulator of ferroptosis (3, 20). Many *in vitro* and *in vivo* studies have shown that the inactivation of GPX4 caused the accumulation of LPO to eventually induce ferroptosis and this type of cell death was entirely suppressed by ferroptosis inhibitor (21–23). In line with these studies, we observed that GPX4 was significantly depleted in myocardial tissue after CA, while the utilization of ferroptosis inhibitor increased GPX4 to approximately 20% of normal levels, which implies that GPX4 could be involved in PRMD.

Ferroptosis targets LPO for executing cell death. Suppression of lipid peroxidation halts the cell death process of ferroptosis (24). Among the many different secondary products during LPO, 4-HNE is the most toxic (25). It causes cardiovascular damage by LPO and other long-lasting biological consequences as second messengers of free radicals, particularly by covalent modification of macromolecules (26). Consistent with these reports, we found that 4-HNE modified proteins significantly accumulated in post-resuscitation cardiac tissue, while UAMC-3203 and DFO could reduce this tendency. Moreover, there was no difference between UAMC-3203 and DFO, but the combined treatment significantly enhanced therapeutic effects in terms of GPX4 and 4-HNE.

The accumulation of excess iron is a fundamental step that contributes to ferroptosis. Our data showed that iron content was increased in heart tissue after resuscitation. There is a sufficiently large number of non-heme iron in the heart tissue, the majority of which merges to ferritin for storage or transferrin for transportation (27, 28). Like other causes of ischemia and reperfusion, CA, and resuscitation released many irons into a transient pool (29). By the Fenton reaction, iron converts hydrogen peroxide to generate ROS, thus damaging the membrane, nucleus, or protein and promoting cell death. Iron chelators, therefore, can be used to inhibit iron-dependent ferroptosis by attenuating iron overload. A recent study by Baba et al. (30) confirmed the presence of iron overload in cardiomyocytes during I/R injury, suggesting the possible role of ferroptosis in IRI. Intriguingly, we have also found that DFO reduced the iron concentration in the myocardium post-CA, but UAMC-3203 was ineffective. This was different from the intervention results on myocardial function, microcirculation, GPX4, and 4-HNE. Mechanistically, as regulative molecules of ferroptosis, UAMC-3203, and DFO target LPO and iron ions respectively, so they have different effects on the iron level. More importantly, this phenomenon also showed that iron might be located at a more upstream position than LPO in the mechanistic chain of ferroptosis. This conjecture is consistent with previous viewpoints (4, 6, 31).

Collectively, based on the appearance of GPX4, 4-HNE, and iron after CPR or treatment with inhibitors, we speculated that the ferroptosis might contribute to PRMD. It also provided a new basis for finding more candidates for the treatment of PRMD. Moreover, compared with two single drugs, the combination has a stronger effect on GPX4 and 4-HNE, but it has no advantage on cardiac function and microcirculation, which likely offers a possibility that ferroptosis is not the only RCD form involved in PRMD. A growing number of studies have demonstrated the relevance of apoptosis (32), mitochondrial-dependent necrosis (33), necroptosis (34), pyroptosis (35), and autophagy (36) with cardiomyocyte death and IRI. Therefore, what types of cell death happened in PRMD, what role it played and whose influence is more crucial are all worth further investigating to help elucidate the pathogenesis.

There are several limitations to this study. First, only rats without underlying diseases were included and the method of administration was an intraperitoneal injection, which is not consistent with clinical situations. Second, this experiment was an exploratory experiment lack of outcome for long-term survival and sufficient researches on the molecular mechanism. Third, morphological analysis was not performed. On the basis of this foundation, further research has been designed and is in progress.

CONCLUSIONS

Our results show that UAMC-3203 or/and DFO improves post-resuscitation myocardial dysfunction and first provided evidence of ferroptosis involvement in PRMD. Ferroptosis inhibitors could potentially be a new therapeutic approach for reducing the severity of myocardial dysfunction caused by CPR.

ACKNOWLEDGMENTS

All work was performed at the Weil Institute of Emergency and Critical Care Research at Virginia Commonwealth University.

REFERENCES

1. Haywood K, Whitehead L, Nadkarni VM, Achana F, Beesems S, Böttiger BW, Brooks A, Castrén M, Ong ME, Hazinski MF, et al.: COSCA (Core Outcome Set for Cardiac Arrest) in adults: an advisory statement from the International Liaison Committee on Resuscitation. *Circulation* 137(22):e783–e801, 2018.

2. Yang M, Chen L, Hua T, Zou Y, Yang Z: Beneficial effects of ivabradine on post-resuscitation myocardial dysfunction in a porcine model of cardiac arrest. *Shock* 53(5):630–636, 2020.
3. Dixon SJ, Lemberg KM, Lamprecht MR, Skouta R, Zaitsev EM, Gleason CE, Patel DN, Bauer AJ, Cantley AM, Yang WS, et al.: Ferroptosis: an iron-dependent form of nonapoptotic cell death. *Cell* 149(5):1060–1072, 2012.
4. Stockwell BR, Friedmann Angeli JP, Bayir H, Bush AI, Conrad M, Dixon SJ, Fulda S, Gascon S, Hatzios SK, Kagan VE, et al.: Ferroptosis: a regulated cell death nexus linking metabolism, redox biology, and disease. *Cell* 171(2):273–285, 2017.
5. Dixon SJ, Stockwell BR: The hallmarks of ferroptosis. *Annu Rev Cancer Biol* 3:35–54, 2019.
6. Xie Y, Hou W, Song X, Yu Y, Huang J, Sun X, Kang R, Tang D: Ferroptosis: process and function. *Cell Death Differ* 23(3):369–379, 2016.
7. Zhao Z, Wu J, Xu H, Zhou C, Han B, Zhu H, Hu Z, Ma Z, Ming Z, Yao Y, et al.: XJB-5-131 inhibited ferroptosis in tubular epithelial cells after ischemia-reperfusion injury. *Cell Death Dis* 11(8):629, 2020.
8. Su L, Jiang X, Yang C, Zhang J, Chen B, Li Y, Yao S, Xie Q, Gomez H, Murugan R: Pannexin 1 mediates ferroptosis that contributes to renal ischemia/reperfusion injury. *J Biol Chem* 294(50):19395–19404, 2019.
9. Li W, Feng G, Gauthier JM, Lokshina I, Higashikubo R, Evans S, Liu X, Hassan A, Tanaka S, Cicka M, et al.: Ferroptotic cell death and TLR4/Trif signaling initiate neutrophil recruitment after heart transplantation. *J Clin Invest* 129(6):2293–2304, 2019.
10. Fang X, Wang H, Han D, Xie E, Yang X, Wei J, Gu S, Gao F, Zhu N, Yin X: Ferroptosis as a target for protection against cardiomyopathy. *Proc Natl Acad Sci U S A* 116(7):2672–2680, 2019.
11. Devisscher L, Van Coillie S, Hofmans S, Van Rompaey D, Goossens K, Meul E, Maes L, De Winter H, Van Der Veken P, Vandenabeele P, et al.: Discovery of novel, drug-like ferroptosis inhibitors with in vivo efficacy. *J Med Chem* 61(22):10126–10140, 2018.
12. Cao JY, Dixon SJ: Mechanisms of ferroptosis. *Cell Mol Life Sci* 73(11–12):2195–2209, 2016.
13. Ye S, Weng Y, Sun S, Chen W, Wu X, Li Z, Weil MH, Tang W: Comparison of the durations of mild therapeutic hypothermia on outcome after cardiopulmonary resuscitation in the rat. *Circulation* 125(1):123–129, 2012.
14. Ma L, Lu X, Xu J, Sun S, Tang W: Improved cardiac and neurologic outcomes with postresuscitation infusion of cannabinoid receptor agonist WIN55, 212-2 depend on hypothermia in a rat model of cardiac arrest. *Crit Care Med* 42(1):e42–e48, 2014.
15. Spronk PE, Ince C, Gardien MJ, Mathura KR, Oudemans-van Straaten HM, Zandstra DF: Nitroglycerin in septic shock after intravascular volume resuscitation. *Lancet* 360(9343):1395–1396, 2002.
16. De Backer D, Hollenberg S, Boerma C, Goedhart P, Büchele G, Ospina-Tascon G, Dobbe I, Ince C: How to evaluate the microcirculation: report of a round table conference. *Crit Care* 11(5):R101, 2007.
17. Yin L, Yang Z, Yu H, Qian J, Zhao S, Wang J, Wu X, Cahoon J, Tang W: Changes in sublingual microcirculation is closely related with that of bulbar conjunctival microcirculation in a rat model of cardiac arrest. *Shock* 45(4):428–433, 2016.
18. Liachenko S, Tang P, Xu Y: Deferoxamine improves early postresuscitation reperfusion after prolonged cardiac arrest in rats. *J Cereb Blood Flow Metab* 23(5):574–581, 2003.
19. Vandebroek A, Yasui M: Regulation of AQP4 in the central nervous system. *Int J Mol Sci* 21(5):1603, 2020.
20. Maiorino M, Conrad M, Ursini F: GPx4, lipid peroxidation, and cell death: discoveries, rediscoveries, and open issues. *Antioxid Redox Signal* 29(1):61–74, 2018.
21. Bai T, Li M, Liu Y, Qiao Z, Wang Z: Inhibition of ferroptosis alleviates atherosclerosis through attenuating lipid peroxidation and endothelial dysfunction in mouse aortic endothelial cell. *Free Radical Biol Med* 160:92–102, 2020.
22. Zhang Z, Wu Y, Yuan S, Zhang P, Zhang J, Li H, Li X, Shen H, Wang Z, Chen G: Glutathione peroxidase 4 participates in secondary brain injury through mediating ferroptosis in a rat model of intracerebral hemorrhage. *Brain Res* 1701:112–125, 2018.
23. Angeli JPF, Schneider M, Proneth B, Tyurina YY, Tyurin VA, Hammond VJ, Herbach N, Aichler M, Walch A, Eggenhofer E: Inactivation of the ferroptosis regulator Gpx4 triggers acute renal failure in mice. *Nat Cell Biol* 16(12):1180–1191, 2014.
24. Gaschler MM, Stockwell BR: Lipid peroxidation in cell death. *Biochem Biophys Res Commun* 482(3):419–425, 2017.
25. Esterbauer H, Eckl P, Ortner A: Possible mutagens derived from lipids and lipid precursors. *Mutat Res* 238(3):223–233, 1990.
26. Ayala A, Munoz MF, Arguelles S: Lipid peroxidation: production, metabolism, and signaling mechanisms of malondialdehyde and 4-hydroxy-2-nonenal. *Oxid Med Cell Longev* 2014:e360438, 2014.
27. Hill JM, Switzer RC 3rd: The regional distribution and cellular localization of iron in the rat brain. *Neuroscience* 11(3):595–603, 1984.
28. Sarco DP, Becker J, Palmer C, Sheldon RA, Ferriero DM: The neuroprotective effect of deferoxamine in the hypoxic-ischemic immature mouse brain. *Neurosci Lett* 282(1–2):113–116, 2000.
29. Lipscomb DC, Gorman LG, Traystman RJ, Hurn PD: Low molecular weight iron in cerebral ischemic acidosis in vivo. *Stroke* 29:487–492, 1998.
30. Baba Y, Higa JK, Shimada BK, Horiuchi KM, Suhara T, Kobayashi M, Woo JD, Aoyagi H, Marh KS, Kitaoka H, et al.: Protective effects of the mechanistic target of rapamycin against excess iron and ferroptosis in cardiomyocytes. *Am J Physiol Heart Circ Physiol* 314(3):H659–H668, 2018.
31. Latunde-Dada GO: Ferroptosis: Role of lipid peroxidation, iron and ferritinophagy. *Biochim Biophys Acta Gen Subj* 1861(8):1893–1900, 2017.
32. Chen Z, Chua CC, Ho YS, Hamdy RC, Chua BH: Overexpression of Bcl-2 attenuates apoptosis and protects against myocardial I/R injury in transgenic mice. *Am J Physiol Heart Circ Physiol* 280(5):H2313–H2320, 2001.
33. Baines CP, Kaiser RA, Purcell NH, Blair NS, Osinska H, Hambleton MA, Brunskill EW, Sayen MR, Gottlieb RA, Dorn GW, et al.: Loss of cyclophilin D reveals a critical role for mitochondrial permeability transition in cell death. *Nature* 434(7033):658–662, 2005.
34. Lee P, Sata M, Lefer DJ, Factor SM, Walsh K, Kitsis RN: Fas pathway is a critical mediator of cardiac myocyte death and MI during ischemia-reperfusion in vivo. *Am J Physiol Heart Circ Physiol* 284(2):H456–H463, 2003.
35. He F, Zheng G, Hou J, Hu Q, Ling Q, Wu G, Zhao H, Yang J, Wang Y, Jiang L, et al.: N-acetylcysteine alleviates post-resuscitation myocardial dysfunction and improves survival outcomes via partly inhibiting NLRP3 inflammasome induced-pyroptosis. *J Inflamm (Lond)* 17(1):1–9, 2020.
36. Posnere B, Tranf KA, Greeng DR, Xavierh RJ, Shawf SY, Clarked PG, Puyald J, Levinea B: Autosis is a Na, K-ATPase-regulated form of cell death triggered by autophagy-inducing peptides, starvation, and hypoxia-ischemia. *Proc Natl Acad Sci U S A* 110(51):20364–20371, 2013.